Int. J. Electrochem. Sci., 10 **(2015)** 7423 - 7439

International Journal of
ELECTROCHEMICAL
SCIENCE
www.electrochemsci.org

Voltammetric Investigation on Uranyl Sorption by Alginate Based Material. Influence of Hydrolysis and pH Dependence

Daniela Piazzese[*], *Salvatore Cataldo, Nicola Muratore*

Dipartimento di Fisica e Chimica, Università degli Studi di Palermo, Viale delle Scienze, I-90128 Palermo, Italy
[*]E-mail: daniela.piazzese@unipa.it

Received: 5 March 2015 / *Accepted:* 24 April 2015 / *Published:* 28 July 2015

The removal of U(VI) as uranyl (UO_2^{2+}) from aqueous solutions was investigated by sorption onto alginate based material. The hydrolysis of uranyl ion was always taken into account in the calculations of free UO_2^{2+} ion in aqueous solution, in the experimental pH range considered, as well as the acid-base properties of alginate polymer. The sorption process follows a pseudo-second order kinetic model and the sorption rate decreases when the pH value increases. In addition to the classical Langmuir and Freundlich models, the equilibrium data were fitted by using a modified multi-component equilibrium model, never tested before. Differential Pulse Voltammetry (DPV) and Inductively Coupled Plasma Optical Emission Spectroscopy (ICP-OES) measurements were carried out in $NaNO_3$ aqueous solutions for the kinetic and equilibrium studies, respectively. Direct measurements of uranyl by DPV were carried out without using complexing agent, as usually reported in the literature; this allowed us to know the free UO_2^{2+} concentration and the hydrolyzed species formed in the ~ 2.0 to 5.0 pH range investigated. The physical structure and morphology of biomaterials was investigated by Scanning Electron Microscopy (SEM) analysis and Energy Dispersive X-ray spectroscopy (EDX) measurements.

Keywords: U(VI) adsorption; pH dependence; low cost biosorption material; kinetic and equilibrium studies; Differential Pulse Voltammetry; ICP-OES measurements;

1. INTRODUCTION

Uranium is the main component of the nuclear fuel and can be considered as one of the most hazardous metal due to its simultaneously radioactive properties and toxicological effects[1]. Owing to the large civil and military use of uranium, especially as depleted uranium[2–8], it is widespread in the

environment under different oxidation states and chemical forms [9–14]. In particular, the uranyl ion UO_2^{2+}, which is the main chemical form of U(VI) in aqueous solution [15,16], shows high toxicity towards living organisms even in trace concentrations [17–20]. According to the environmental protection agency (US EPA) a maximum uranium contaminant level of 30 μg L^{-1} is accepted for aqueous ecosystems [21]. Therefore, for the environmental safety assessment and for the protection of human health a chemical process able to reduce the uranyl concentration in aquatic ecosystem and wastewaters is needed. To this end, we report here the results of an investigation on the uranyl ion removal from aqueous solutions by sorption onto low cost and environmental friendly alginate based material in gel phase, already tested successfully for different heavy metals removal [22–25]. The study has been performed by kinetic and equilibrium measurements by taking into account the chemical behaviour of both the sorbent material (acid-base properties, metal complex formation, availability of binding groups) and the metal ion (its tendency to hydrolyze and to react with ligands), with the aim to assess the best conditions (pH, ionic strength and medium composition) to obtain the highest removal efficiency. Few papers are reported in the literature on the uranium removal by alginate [26] and alginate composite [27] or by nonliving algal biomass [28,29] In all the cases, spectroscopic ICP and/or UV-Vis. measurements were carried out to evaluate the uranium concentration in solution during batch kinetic experiments. In this paper the uranyl concentration in solution has been evaluated by direct Differential Pulse Voltammetry (DPV) measurements which allowed us to check in continuous the solution concentration of uranyl in the pH range investigated, taking into account the presence of both free and hydrolyzed uranium(VI) species (details are in § 4.2.2). Alginate biosorbent has been chosen because it is a very low cost and available material, being alginic acid the main component of brown algae where it is present up to 40% dry weight [30]. From the chemical point of view, alginic acid is an acidic polysaccharide constituted by monomer units of mannuronic and guluronic acids [31,32] containing carboxylic binding groups being able to react, in their deprotonated form, with several metal ions including uranyl ion [33], to form stable complexes. On the other hand, uranyl ion shows a strong tendency to hydrolyse in aqueous solution with the formation of mono and polynuclear species [34,35], according to the following equation

$$pUO_2^{2+} + qH_2O = (UO_2)_p(OH)_q^{(2p-q)} + qH^+ \qquad (1)$$

with (p,q) = (1,1), (2,2), (3,4), (3,5), (3,7).

The formation of uranyl hydrolyzed species could lower the free uranyl ion concentration by reducing the sorption efficiency onto alginate. For the above reasons, the conditions of pH have been accurately investigated in order i) to have an adequate amount of deprotonated carboxylic groups, being able to interact with uranyl ion, and ii) to exclude the formation of uranyl hydrolyzed species. Therefore, kinetic and equilibrium measurements were carried out in $NaNO_3$ 0.1 mol L^{-1} in acidic pH range (2.5 < pH < 5.5) using different uranyl/ biomaterial mass ratios. Among the different models considered to explain the kinetic data, the best fit for the system under investigation was obtained using the pseudo second order model which is generally the most used one to describe the sorption process when the chemical sorption is the rate - controlling step [36,37]. In order to better explain the

experimental multi-step curves obtained in this investigation, the equilibrium data were fitted by using a modified multi-component equilibrium model, never tested before, obtained considering different mathematical approaches [38]. The residual concentration of uranyl ion in aqueous solution during kinetic measurements and equilibrium investigation was determined by Differential Pulse Voltammetry (DPV) and Inductively Coupled Plasma Optical Emission Spectroscopy (ICP-OES), respectively. The physical structure and morphology of biomaterials were investigated by Scanning Electron Microscopy (SEM) analysis and Energy Dispersive X-ray spectroscopy (EDX) measurements.

2. REAGENTS AND MATERIALS

2.1. Reagents

Alginic acid (AA, M_w = 70-100 kDa), as sodium salt extracted from *Macrocystis pyrifera*, with an average content of mannuronic and guluronic acids of 61% and 39%, respectively, was supplied by Sigma (lot. 60K1443). Dioxo-uranium (VI) cation (UO_2^{2+}) was used as nitrate salt (Fluka). The purity of dioxo-uranium (VI) nitrate, checked gravimetrically after precipitation as U_3O_8 by gaseous ammonia, was > 99.5 %. All solutions were prepared using milliQ pure water and class A glassware

2.2. Preparation of sorbent material

Alginate based material was prepared as calcium alginate gel beads (Ca-A) with an alginate content of 2% using a dropping technique previously tested successfully [22,23,39]. In particular, a peristaltic pump (GILSON, Minipuls 3) was used to dispense the suspension in a stirred reservoir containing 200 mL of a $CaCl_2$ 0.1 M solution used for gel formation. At the end of the dispensing tube a micropipette tip (type 20–200 μL) cut out to get a final diameter of 1 mm was attached and positioned approximately 1 cm above the surface of the fixing solution. The beads formed were allowed to cure, under continuous stirring, in the same $CaCl_2$ solution for 24 h; they were rinsed three times with distilled water to ensure the removal of unbound calcium ion.

3. PROCEDURES AND METHODS

3.1. Characterization of gel beads

The structure and morphology of Ca-A gel beads were investigated by SEM technique using an electronic microscope ESEM FEI QUANTA 200F coupled with an EDX (Energy Dispersive X-ray spectroscopy) system. To evaluate the eventual change in morphology due to the uranyl adsorption, measurements were carried out before and after uranyl adsorption using 25 gel beads (the average weight of 25 beads is equal to 17,5mg [22]) in 0.1 mol L^{-1} of $NaNO_3$ and in ~170 ppm of UO_2^{2+}

solution, in the same ionic medium at pH = 4.2, respectively. Before analysis, gel beads were dried at t = 105 °C in oven and their surface was coated with gold in the presence of argon by an Edwards Sputter Coater S150A in order to prevent charging under electronic beam. The electron beam was opportunely set in order to avoid the damage of the samples. SEM micrographs were registered within the micrometer range.

Results from SEM and EDX analysis are reported in Figs. 1a-d. As can be seen, the presence of UO_2^{2+} (Figure 1b) causes a more irregular structure and morphology of the calcium alginate surface, in accordance with recent investigations [40], with the formation of wrinkles and flakes, giving evidence for the uranyl sorption by the biomaterial. Results obtained from EDX measurements before (Figure 1c) and after (Figure 1d) UO_2^{2+} sorption show a much higher content of calcium ion in solution when the biopolymer is in contact with uranyl ion. This let us to suppose that a possible adsorption mechanism is due to the exchange between the calcium of alginate gel and the uranyl present in solution with the formation of stable uranyl-alginate complexes, as already registered for other alginate metal systems [22,40,41].

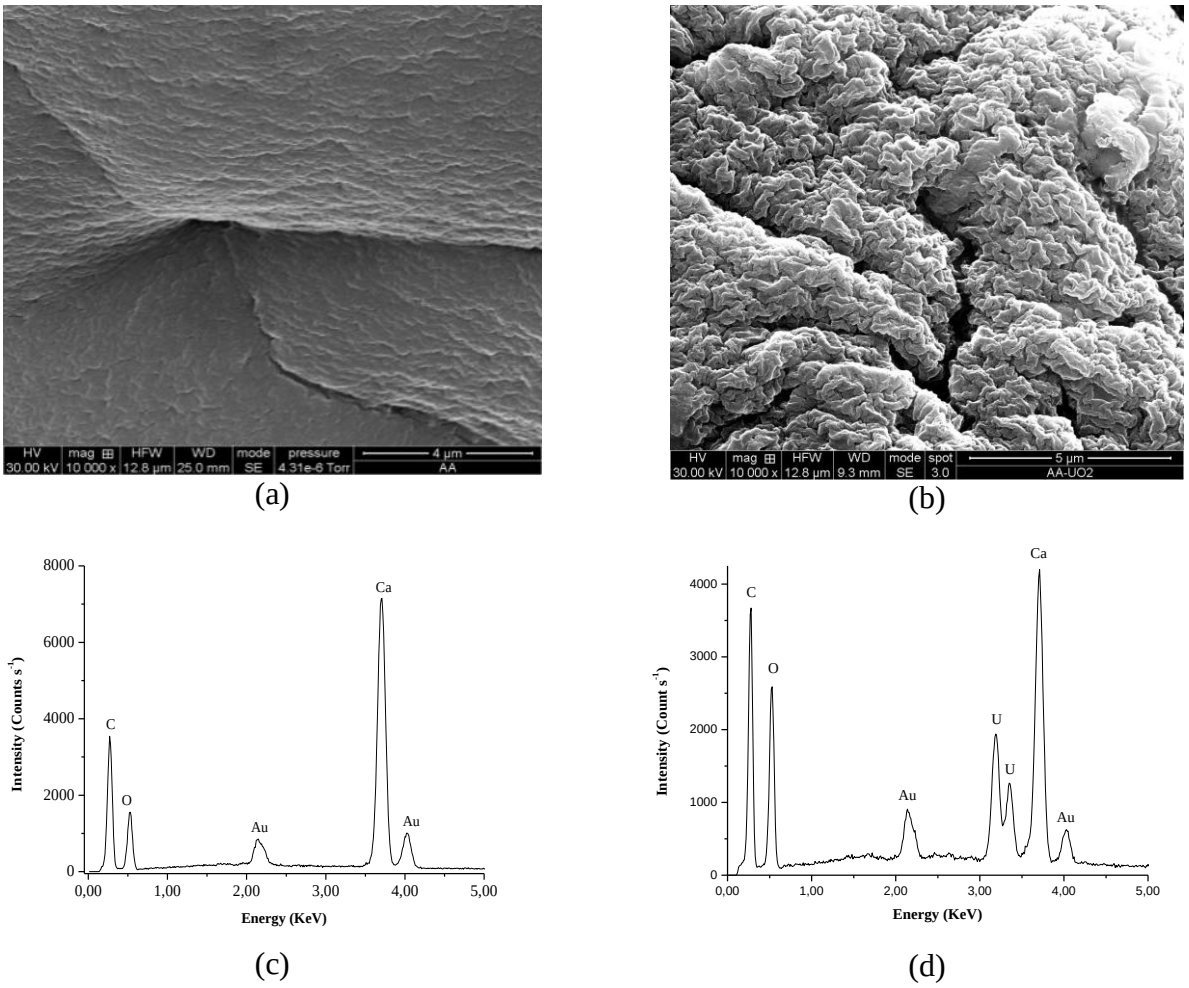

Figure 1. SEM images at 10000x magnification of Ca-A gel bead surface before (a) and after (b) sorption of UO_2^{2+} ions; EDX spectra of Ca-A (c) and Ca-A/ UO_2^{2+} (d).

3.2. Procedures for kinetic investigations.

The kinetic investigations were performed in continuous evaluating, by Differential Pulse Voltammetry (DPV), the residual UO_2^{2+} concentration in the solution after the sorption process by calcium alginate gel beads. Measurements were carried out on 25 mL of aqueous solution containing ~ 50 mg L^{-1} of UO_2^{2+} and 25 gel beads of sorbent material, at room temperature and 0.1 mol L^{-1} ionic strength ($NaNO_3$). The polarographic apparatus was a Metrohm 663 VA STAND controlled by the Autolab potentiostat in conjunction with the IME663 interface. The VA STAND was equipped with a three electrode system consisting of a Multi Mode Electrode Pro (Metrohm, code 6.1246.120) working in the Static Mercury Drop Electrode (SMDE) mode, a glassy carbon auxiliary electrode (code 6.1247.000) and a double junction Ag/AgCl/KCl (3 mol L^{-1}) reference electrode (code 6.0728.030).

In order to check for the pH change during the kinetic absorption process ISE-H^+ measurements were simultaneously carried out by interfacing a potentiometric apparatus to a polarographic system. ISE-H^+ measurements were carried out using a 809 Metrohm *Titrando* apparatus equipped with a combined glass electrode (code 6.0258.010). The whole electrochemical apparatus was controlled by NOVA 1.6 and Metrohm *TiAMO* 2.0 software. The DPV measurements were carried out under the experimental electrochemical conditions shown in Table 1.

Table 1. Experimental electrochemical conditions

Parameter	
Deposition potential	0.05V
Deposition time	1 s
Equilibration time	5 s
Potential interval	0.05 / -0.3 V
Scan rate	0.008 V s^{-1}
Step potential	-4 mV
Modulation amplitude	-50 mV
Modulation time	0.1 s
Time interval	0.5 s

The peak current of UO_2^{2+} was recorded every 3.5 minutes during the first 10 minutes and every 6 minutes in the remaining time. The experimental electrochemical conditions were chosen in order to optimize the quality parameters, as signal/noise ratio, repeatability, accuracy, etc.; Voltammetric calibration curves (details in the § 4.2.2. Analysis of free uranyl ion in solution) were drawn by measuring the variation of I_{max} in the pH range considered at different uranyl concentrations ($3.7\times10^{-6} < C_{(U(VI)} < 1.8\times10^{-4}$ mol L^{-1}).

Metal adsorption at different contact times t (q_t, mg g^{-1}) was calculated considering:

$$q_t = \frac{V(C_0 - C_t)}{g_{dry_{beads}}} \quad (2)$$

where V, C_0 and C_t are the volume and the metal concentration in solution expressed as mg L^{-1} at t = 0 and t = t, respectively.

3.3. Procedures for adsorption at equilibrium conditions

To investigate the uranyl adsorption at equilibrium conditions, the residual concentration of UO_2^{2+} in solution was determined in different aliquots of 25 mL of solution, at 0.1 mol L^{-1} ionic strength and at pH = 4.2, containing 170 mg L^{-1} of uranyl ion and an increasing amount, from 1 to 100, of gel beads. Before analysis the solutions were stored in 50 ml conical flasks and shaken in an orbital shaker at constant rate (140 rpm) for 24 hours at room temperature. The residual concentration of UO_2^{2+} in solution was determined by ICP-OES measurements.

4. RESULTS AND DISCUSSION

The sorption process mechanism is based on the possibility that uranyl ion present in solution interacts with carboxylic binding groups of polymer biomaterials to form stable species. In order to facilitate this interaction and to obtain the best metal sorption efficiency, the more suitable conditions of solutions containing the dioxouranium(VI) cation to be removed were assessed on the basis of acid-base properties of alginate polymer and uranyl ion in aqueous solution.

4.1. Acid base properties of alginate biopolymer

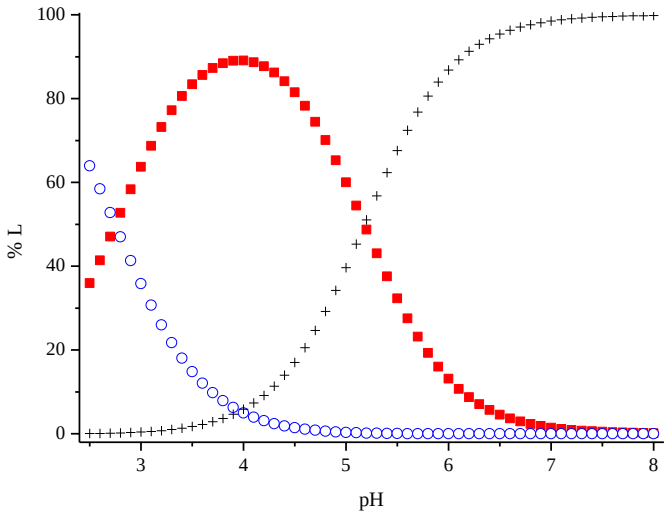

Figure 2. Distribution diagram of alginate species [AAH (■); AAH_2(○); AA^{2-}(+)], at 0.1 mol L^{-1} ionic strength in Na^+ ionic medium, at 25 °C.

Acid-base properties of alginic acid (AA) have been previously investigated [42,43] using different models. According to the so called "diprotic like model" [43], the proton exchange capacity of the biopolymer in all the acid pH range can be defined by only two protonation constants: $\log K_1^H$ = 3.499 and $\log \beta_2^H$ = 6.421, at 0.1 mol L^{-1} ionic strength [43]. Therefore, according to this model, alginic acid can be present, in the different pH ranges, as diprotonated (AAH_2), monoprotonated (AAH) and fully deprotonated (AA) species, as shown in the distribution diagram reported in Figure 2. As can be seen, the monoprotonated and un-protonated species of alginate, useful to the interaction with uranyl ion, are present, at different percentage formation, in the pH range 3 to 8. In particular, the maximum percentage formation of mono-protonated species is at pH ~ 4 and 100% formation of unprotonated species is registered over pH 6.

4.2. Speciation and analysis of uranyl ion

4.2.1. Hydrolysis speciation of uranyl

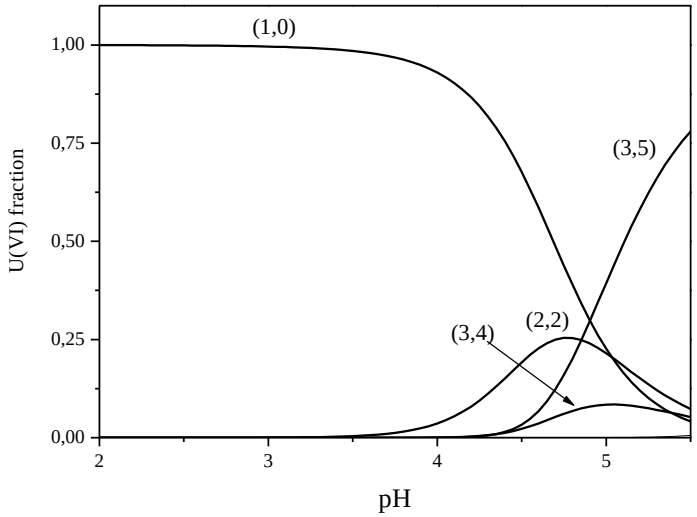

Figure 3. Speciation diagram for the hydrolysis of UO_2^{2+} in $NaNO_3$ 0.1 mol L^{-1} at 25°C [$C_{UO_2^{2+}} = 1.8\times10^{-4}$ mol L^{-1}]. Indexes refer to the stoichiometric coefficients according to the eq.(1).

The strong tendency to hydrolyze of uranyl cation in aqueous solution is well known [15,16,34]. As pointed out before (see Introduction section), the formation of different mononuclear and polynuclear hydrolyzed species of uranyl ion (see eq. 1) can lead to a lowering of the free UO_2^{2+} concentration, with a consequent reduced interaction with carboxylic binding sites of alginate. Therefore, the pH conditions corresponding to the highest percentage formation of free uranyl ion must be assessed. Using the hydrolysis constants reported in the literature [34,35] we report, in Figure 3, the

distribution of the hydrolyzed species of UO_2^{2+} as function of pH in the experimental conditions here adopted [$NaNO_{3(aq)}$ = 0.1 mol L^{-1}, $C_{UO_2^{2+}}$ = 1.8×10^{-4} mol L^{-1}, t = 25°C]. As can be seen, the free uranyl ion is the main species in the acidic pH range 2.5 < pH < 4.5. In particular, at pH 4.5 it is present at about 70% formation. Over pH 5 the formation of the $[(UO_2)_3(OH)_5]^+$ hydrolyzed species is registered. The results obtained by the speciation studies on the alginate protonation and the uranyl hydrolysis let us to affirm that a pH near to 4.5 is to be considered in order to have contemporary an adequate amount of interacting carboxylate sites in alginate biopolymer and a fairly high concentration of free uranyl ion. Therefore, the pH = 4.2 has been chosen as the best value to perform adsorption measurements at equilibrium conditions.

4.2.2. Analysis of free uranyl ion in solution

The speciation study of uranyl ion has been experimentally verified by Differential Pulse Voltammetry (DPV) analysis of the ion in solution during the kinetic measurements, by exploiting the reduction reaction (3)

$$UO_2^{2+}(VI) + e^- \rightarrow UO_2^{+}(V) \qquad (3)$$

The results obtained are summarized in Figures 4 and 5 where the trends of peak potential E_p (V) and peak current i_p (A) are shown, respectively, as a function of pH and for different uranyl ion concentrations.

The results indicate clearly that uranyl is present as free species UO_2^{2+}(VI) up to pH ~ 4.5 and reduces to UO_2^{+}(V) (eq. 3) reversibly with a peak potential E_p = -0.13 V (Fig. 2); for pH values over 4.5, peak potential shifts towards more negative values, evidently owing to the formation of uranyl hydrolyzed species which causes interference on the electrode surface.

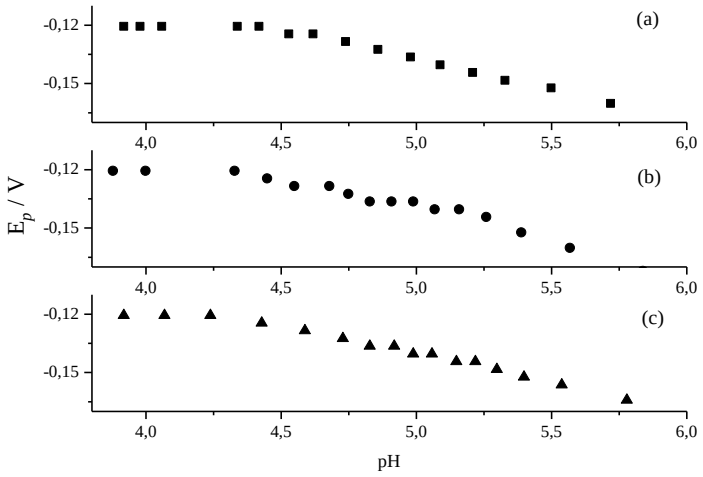

Figure 4. Peak potential E_p (V) *vs.* pH. C(UO_2^{2+})/mol L^{-1}: (a) $3.7x10^{-5}$, (b) $1.1x10^{-4}$; (c) $1.8x10^{-4}$

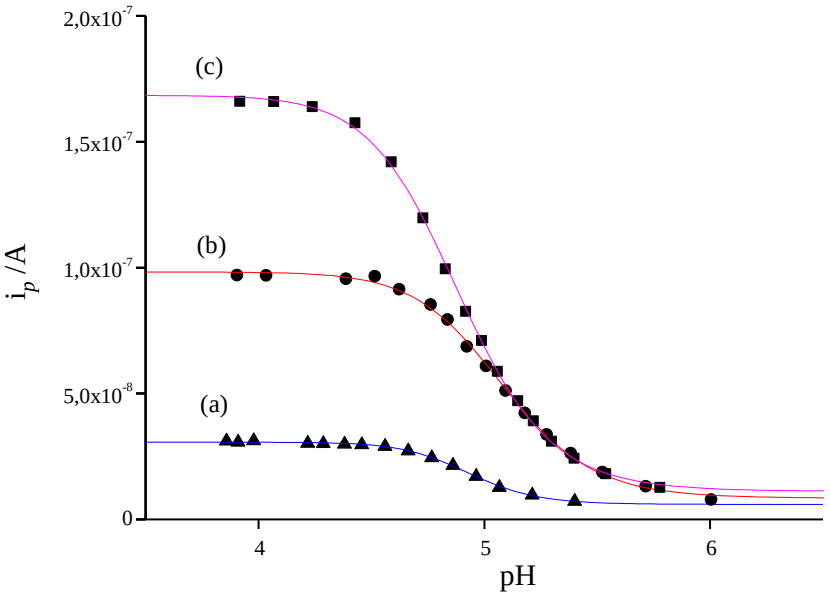

Figure 5. Peak current i_p (A) *vs.* pH. C(UO_2^{2+})/mol L^{-1}: (a) $3.7x10^{-5}$, (b) $1.1x10^{-4}$; (c) $1.8x10^{-4}$.

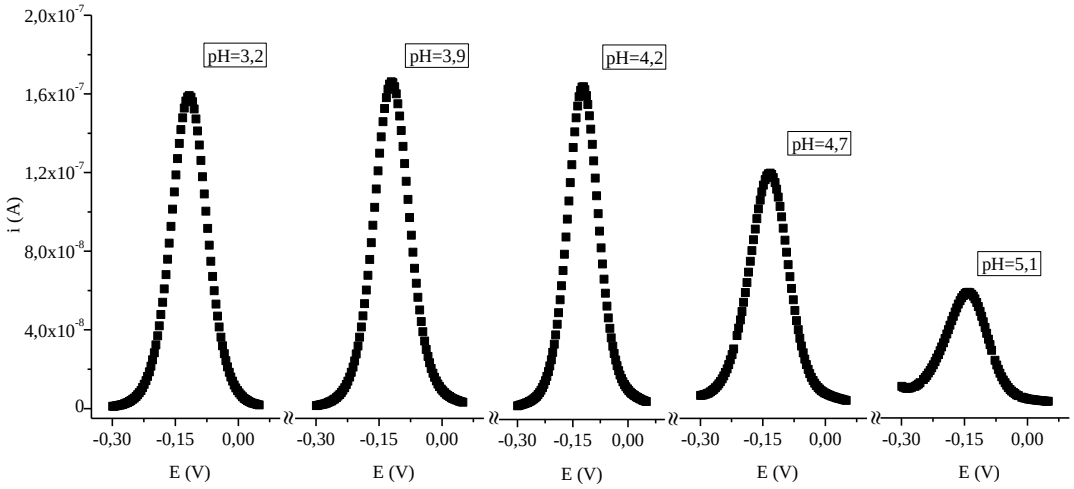

Figure 6. Current, i(A) *vs.* potential E(V) in the pH range 3 - 5

Peak current curves (Fig. 5) are fitted as a function of pH by using the sigmoidal equation $y = A + (B - A)/1 + (x/x_0)^p$ with the following empirical parameters: curve (a): A = $6x10^{-9}$; B = $3x10^{-8}$; x_0 = 5.17; p = 29.4; curve (b): A = $9.8x10^{-9}$; B = $8.4x10^{-8}$; x_0 = 4.98; p = 26.9; curve (c): A = $1x10^{-8}$; B = $1.7x10^{-7}$; x_0 = 4.89; p = 24.3. As can be seen the peaks current i_p increase regularly as the uranyl ion concentration increases for pH values < 4.5. This trend is in agreement with the results obtained by speciation analysis of uranyl ion (see § 4.2.1) according to which below pH ~ 4.5 the uranyl is present mainly as free UO_2^{2+} species and there is no interference at the mercury electrode surface by hydrolyzed species. At pH values higher than 4.5 the concentration of free UO_2^{2+} in solution decreases

rapidly so much that it becomes negligible and the relative current peaks tend to disappear. Figure 6 shows the current peak as a function of potential at five pH values in the range 3 to 5. As can be seen, the current peak at pH = 4.2 is very close to the current peak values obtained in the acidic pH range where hydrolyzed species are not present at all.

The results obtained by DPV measurements are in very good agreement with findings by speciation analysis and allow us to confirm that the pH = 4.2 is the best one to have uranyl ion as free species being able to interact with carboxylic binding sites of alginate. Moreover, it must be noted that the preventive knowledge of pH range where no hydrolysis occurs (see speciation analysis) allowed us to carry out DPV measurements without using chloroanilic acid (2,5-dichloro-3,6-dihydroxy-1,4-benzoquinone) as complexing agent for uranyl ion as recommended by some authors in order to inhibit the hydrolysis of the cation [44].

4.3 Kinetic results

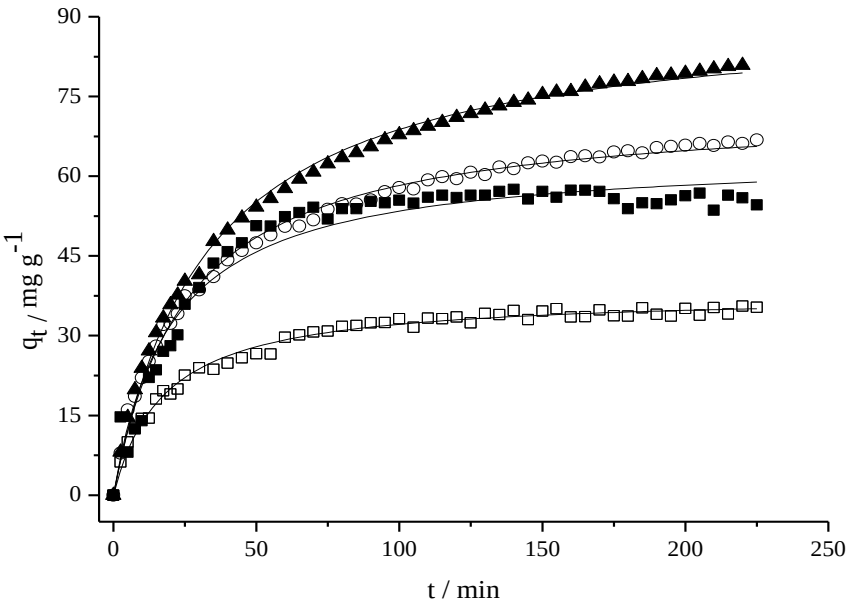

Figure 7. Pseudo second order kinetic trend of UO_2^{2+} / Ca-A gel beads systems at different initial pH values [pH = 4.17 (▲); pH = 2.83 (○); pH = 5.36 (■); pH = 2.34 (□)].

Different models such as pseudo first order, double exponential model and Higuchi and Weibul models [45,46], have been used to explain the kinetic data. Among the different models tested, the best fit was obtained using a pseudo second order law expressed by the eq. 4, which is reported in its integrated form [boundary conditions (t = 0 to t = t and q_t = 0 to q_t = q_t)]:

$$q_t = \frac{t}{\frac{1}{k_2 q_e^2} + \frac{t}{q_e}} \qquad (4)$$

where q_e and q_t represent the amount of metal ion adsorbed (mg g^{-1}) at equilibrium and at different contact times (t), respectively; k_2 is the pseudo-second order rate constant (mg^{-1} min^{-1} g). By fitting the experimental kinetic data to eq. 4, (Figure 7) the second order rate constant k_2 and q_e are determined in the pH range investigated (2.3 < pH < 5.4). The experimental trend of both these parameters as function of pH is reported in Figures 8(a,b). Figure 8(a) shows, as expected, that the maximum sorption of uranyl ion (91.2 mg g^{-1}) is at pH ~ 4.2, confirming once again that this pH value is the most appropriate to make possible the interaction between free uranyl and alginate in its partially deprotonated form.

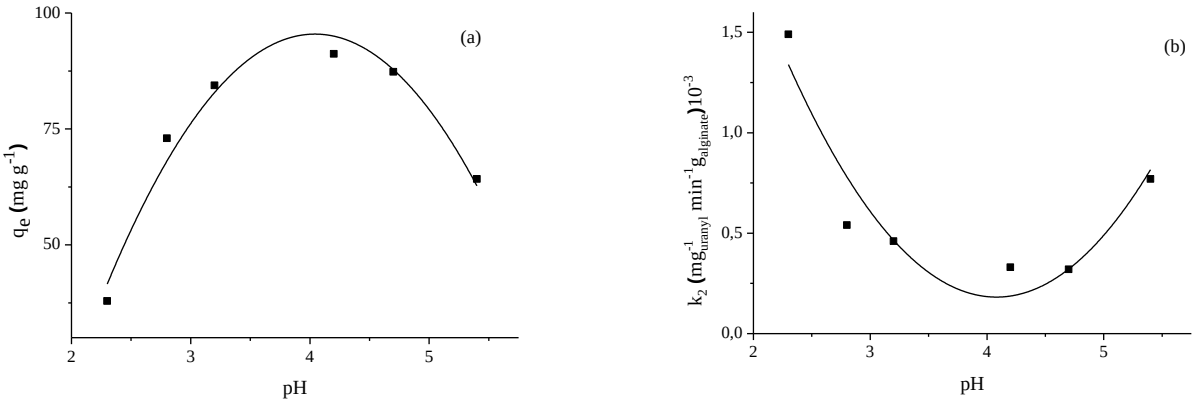

Figure 8. Dependence of q_e (a) and k_2 (b) [according to eq.(4)] on pH, at room temperature.

As concerns the rate of the process, data reported in Figure 8(b) show that the kinetic constant values k_2 depend strongly on the solution pH; k_2 values decrease regularly as pH values increase and reach a minimum at pH ~ 4.5 where the maximum adsorption of uranyl ion by alginate occurs.

4.4 Equilibrium results

The equilibrium adsorption data were preliminary fitted by Langmuir and Freundlich equations [47]. Moreover, to better understand the experimental multi-step curve obtained in this experimental investigation, the following alternative Competitive Adsorption isothermal Model (CAM) was also used by taking into account the different mathematical models reported by some authors [38,48]:

$$M + S \rightleftharpoons MS \qquad r_1$$
$$nM + S \rightleftharpoons M_nS \qquad r_2$$

where M is the uranyl ion in solution, S is the carboxylic binding sites ($-COO^-$ = S) on polymer surface and n is an empirical parameter which accounts for the formation of mono- (MS) and polynuclear (M_nS) complex species. For the above equilibrium reactions we may define the corresponding adsorption equilibrium constants k'_1 and k'_2 reported in eqs. 5 and 6

$$k_1' = \frac{[MS]}{[M]\times[S]} \quad \text{eq. (5)}$$

$$k_2' = \frac{[M_nS]}{[M]^n\times[S]} \quad \text{eq. (6)}$$

By considering the mass balance equations for the uranyl ion (M) and the sorbent material (S), [eqs. (7) and (8)],

$$C_M = [M]+[MS]+n[M_nS] \quad \text{eq. (7)}$$

$$C_S = [S]+[MS]+[M_nS] \quad \text{eq. (8)}$$

and the sorbate/sorbent concentration ratio (eq. 9),

$$\frac{q_e}{q_L} = \frac{C_M - [M]}{C_S} \quad \text{eq. (9)}$$

we can rearrange eq. (9) to obtain

$$q_e = \frac{q_L\left(k_1C_e + nk_2C_e^{\,n}\right)}{1+k_1C_e+k_2C_e^{\,n}} \quad \text{eq. (10)}$$

where C_e is the equilibrium concentration of the uranyl ion.

Equilibrium adsorption data treatment are shown in Figure 9.

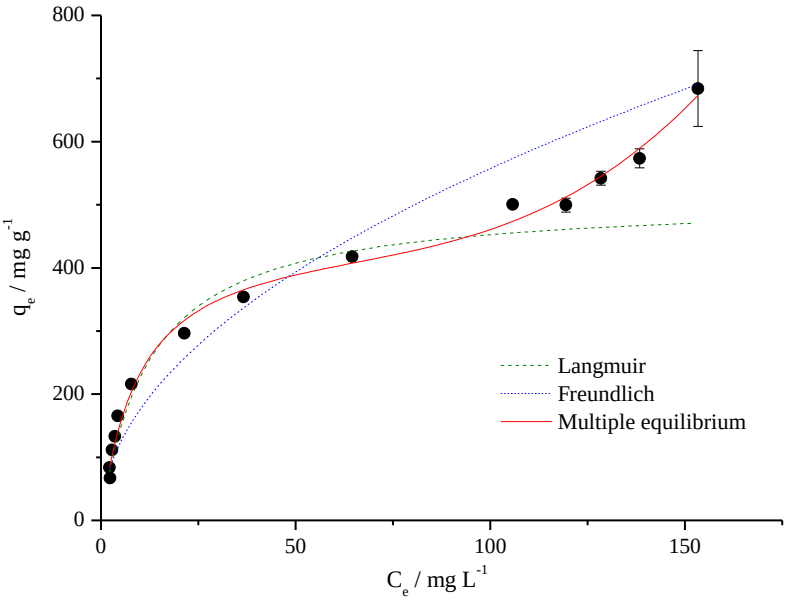

Figure 9. Adsorption isotherms plot of UO_2^{2+} at room temperature. Experimental conditions: pH = 4.2; initial metal concentration 170 mg L^{-1}; contact time: 24 hours.

The assumptions here made are supported by considering that for $2 \leq C_e$ /mg $L^{-1} \leq 40$, corresponding to a number of beads (N_B) in the range $20 < N_B \leq 100$ an equimolar ratio metal to ligand is established and the formation of a mononuclear complex species is correctly justified; for $C_e \geq 40$ mg L^{-1} corresponding to $1 \leq N_B < 20$, the metal to ligand concentration ratio is > 1 and the formation of polynuclear complex species is more likely. The results obtained by fitting data to eq. (10) were reported in Tab. 2. A comparison between k_1 and k_2 values gave evidence for a more probable formation of a mononuclear species MS; as can be seen, the experimental data of the second part of the curve (for $C_e > 100$ mg L^{-1}), do not reach, as expected, the theoretical plateau: this is probably due to the minimum amount of beads used ($N_B = 1$) which causes large errors in k_2 and n values. For this reasons, in order to confirm our assumptions, we analyzed experimental data with the most used single-component isotherm model, *i.e.* the Langmuir model [eq. (11)]. The results are reported in Table 2 together with those obtained by Competitive Adsorption Model (CAM).

$$q_e = \frac{q_L k_L C_e}{1 + k_L C_e} \qquad \text{eq. (11)}$$

Table 2. Sorption isotherm parameters of Uranium (VI) by alginate based material at room temperature

Competitive Adsorption model		Langmuir model	
q_L [a]	464±24 [d]	q_L [a]	509±53 [c]
k_1 [b]	0.10±0.01	k_L [b]	0.08±0.01
k_2 [c]	$3\times10^{-12}\pm1.6\times10^{-11}$	R^2	0.9282
n	5.4±0.9		
R^2	0.9923		

[a] mg g^{-1}; [b] L mg^{-1}; [c] L^n mg^{-n}; [d] std. dev.

As can be seen q_L and k_L values by the Langmuir model are comparable, within the experimental errors, with q_L and k_1 values achieved by the CAM. But, despite ~~of~~ this accordance, Langmuir isotherm model is not able to effectively describe the equilibrium data corresponding to higher values of C_M/C_S ratio; furthermore, considering the correlation coefficient values R^2 for both models, the Competitive Adsorption model seems to fit the equilibrium data better than Langmuir model.

4.5. Hypothesis of sorption mechanism

To verify our hypothesis according to which the main sorption mechanism occurs via cation exchange between calcium ion of calcium alginate gel beads and the uranyl ion present in solution, the amount of calcium release during sorption experiments has been also evaluated by ICP measurements. The results are shown in Figure 10, where the kinetics of uranyl sorption and calcium release is reported together for comparison.

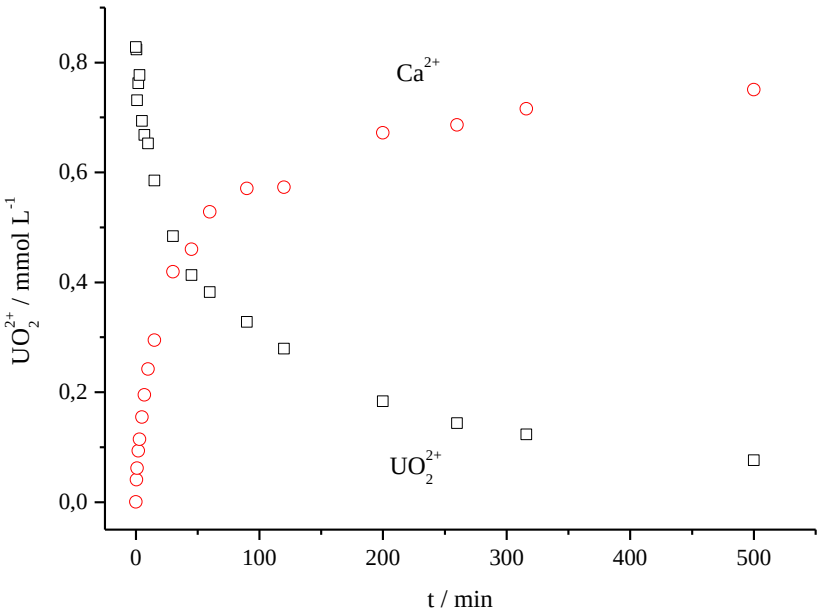

Figure 10. Kinetics of UO_2^{2+} sorption [mmol L^{-1} of UO_2^{2+} in solution; (□)] and Ca^{2+} released [mmol L^{-1} of Ca^{2+} in solution; (●)] by alginate gel beads, at room temperature and pH = 4.2

As can be seen, a good accordance can be noted between the amount of uranyl adsorbed and the calcium ion released. The comparative trend, expressed as q_t (mmol g^{-1}) of uranyl adsorption and calcium release at equilibrium conditions, shown in Figure 11, confirms that an effective uranyl/calcium exchange occurs at equilibrium conditions. Furthermore experimental data fitted by linear equation show a slope line value of 0.9595.

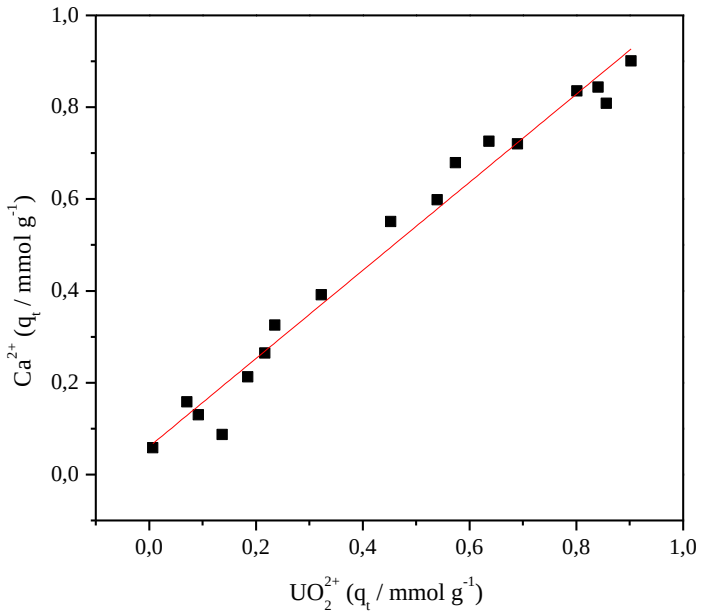

Figure 11. Comparative trend, expressed as q_t (mmol g^{-1}) of uranyl adsorbed and calcium released by alginate gel beads.

The results obtained support our hypothesis according to which the main sorption mechanism occurs, as for other systems till now investigated [22,23,39], through an ion exchange between the metal ion to be removed from the solution (in this case, the dioxouranium(VI) cation) and the calcium of calcium alginate gel beads.

5. CONCLUSIONS

Alginate based material was used in gel phase for uranyl ion removal from aqueous solutions and the process was estimated on the basis of kinetic and equilibrium studies. Physical and mechanical properties of this sorbent was characterized by different techniques, such as SEM - EDX, DPV and ICP-OES can be considered an appropriate experimental technique to perform kinetic investigations as it allows direct measurements of uranyl ion concentration without using complexing agent, as usually reported in the literature.

The results of preliminary speciation analysis allowed us to assess the pH value of about 4.2 as the most appropriate one a) to avoid or minimize the hydrolysis of metal ions under investigation as well as the protonation of alginate, b) to make possible the interaction between free uranyl and alginate in its partially deprotonated form and c) to favor the formation of stable metal-biopolymer complex species. The results obtained from kinetic and equilibrium investigations show that: a) the removal of uranyl ions from the solution occurs prevalently by ion exchange with calcium ion present in the gel beads and relevant relationships were found between the amount of UO_2^{2+} absorbed and the Ca^{2+} released; b) the sorption ability of alginate based material strongly depends on the solution pH; c) the sorption process follows a pseudo second-order kinetic model and the sorption capacity achieves the highest value (91.2 mg g^{-1}) at pH ~ 4.2; d) the Competitive Adsorption isothermal Model (CAM) fits equilibrium adsorption data better than the Freundlich and Langmuir models.

ACKNOWLEDGEMENTS.
The authors carried out this work thanks to a grant from the project ‘‘Development of innovative technologies for the treatment of fluid wastes from shipping activities and for marine environment protection’’ (PON02_00153_2849085 ‘‘Ricerca e competitività 2007-2013, asse 1’’).

References

1. T. Mathews, K. Beaugelin-Seiller, J. Garnier-Laplace, R. Gilbin, C. Adam, C. Della-Vedova, *Environ. Sci. Technol.* 43 (2009) 6684.
2. C.M. Alexandra, Depleted Uranium: Properties, Uses, and Health Consequences, CRC Press, 2006.
3. A. Bleise, P.R. Danesi, W. Burkart, *J. Environ. Radioact.* 64 (2003) 93.
4. E. Craft, A. Abu-Qare, M. Flaherty, M. Garofolo, H. Rincavage, M. Abou-Donia, *J. Toxicol. Environ. Health B Crit. Rev.* 7 (2004) 297.
5. J.L. Domingo, *Reprod. Toxicol. Elmsford N* 15 (2001) 603.
6. C. Giannardi, D. Dominici, *J. Environ. Radioact.* 64 (2003) 227.
7. J. Patocka, J. Kassa, R. Stetina, G. Safr, J. Havel, *J. Appl. Biomed.* 2 (2004) 37.

8. The Royal Society Working Group on the Health Hazards of Depleted Uranium, *J. Radiol. Prot.* 22 (2002) 131.
9. D. Ribera, F. Labrot, G. Tisnerat, J.F. Narbonne, *Rev. Environ. Contam. Toxicol.* 146 (1996) 53.
10. A. Meinrath, P. Schneider, G. Meinrath, *J. Environ. Radioact.* 64 (2003) 175.
11. Q.H. Hu, J.Q. Weng, J.S. Wang, *J. Environ. Radioact.* 101 (2010) 426.
12. W. Luo, B. Gu, *Environ. Sci. Technol.* 43 (2009) 152.
13. I.W. Oliver, M.C. Graham, A.B. MacKenzie, R.M. Ellam, J.G. Farmer, *Environ. Sci. Technol.* 42 (2008) 9158.
14. S. Kerisit, C. Liu, *Geochim. Cosmochim. Acta* 74 (2010) 4937.
15. I. Grenthe, H. Wanner, Chemical Thermodynamics of Uranium, OECD Nuclear Energy Agency - North-Holland, 1992.
16. R. Guillaumont, T. Fanghänel, J. Fuger, I. Grenthe, V. Neck, D.A. Palmer, M.H. Rand, Update on the Chemical Thermodynamics of Uranium, Neptunium, Plutonium, Americium and Technetium, Volume 5, 1 edition, Elsevier Science, Amsterdam ; Boston : Paris, 2003.
17. M.L. Zamora, B.L. Tracy, J.M. Zielinski, D.P. Meyerhof, M.A. Moss, *Toxicol. Sci.* 43 (1998) 68.
18. D. Muller, P. Houpert, J. Cambar, M.-H. Hengé-Napoli, *Toxicol. Appl. Pharmacol.* 214 (2006) 166.
19. M. Ozmen, M. Yurekli, *Environ. Toxicol. Pharmacol.* 6 (1998) 111.
20. R.B. Harvey, L.F. Kubena, S.L. Lovering, H.H. Mollenhauer, T.D. Phillips, *Bull. Environ. Contam. Toxicol.* 37 (1986) 907.
21. USEPA Washington DC, (1996).
22. S. Cataldo, A. Gianguzza, A. Pettignano, I. Villaescusa, *React. Funct. Polym.* 73 (2013) 207.
23. S. Cataldo, G. Cavallaro, A. Gianguzza, G. Lazzara, A. Pettignano, D. Piazzese, I. Villaescusa, *J. Environ. Chem. Eng.* 1 (2013) 1252.
24. S. Cataldo, A. Gianguzza, M. Merli, N. Muratore, D. Piazzese, M.L. Turco Liveri, *J. Colloid Interface Sci.* 434C (2014) 77.
25. G. Cavallaro, A. Gianguzza, G. Lazzara, S. Milioto, D. Piazzese, *Appl. Clay Sci.* 72 (2013) 132.
26. C. Gok, S. Aytas, *J. Hazard. Mater.* 168 (2009) 369.
27. A. Tayyebi, A. Khanchi, M.B. Ghofrani, M. Outokesh, *Sep. Sci. Technol.* 45 (2010) 288.
28. M.H. Khani, A.R. Keshtkar, B. Meysami, M.F. Zarea, R. Jalali, *Electron. J. Biotechnol.* 9 (2006) 100.
29. A. Günther, J. Raff, G. Geipel, G. Bernhard, *Biometals Int. J. Role Met. Ions Biol. Biochem. Med.* 21 (2008) 333.
30. Kelco (Firm), Alginate Products for Scientific Water Control., Kelco, [San Diego, Calif.], 1987.
31. T.A. Davis, F. Llanes, B. Volesky, G. Diaz-Pulido, L. McCook, A. Mucci, *Appl. Biochem. Biotechnol.* 110 (2003) 75.
32. T.A. Davis, F. Llanes, B. Volesky, A. Mucci, *Environ. Sci. Technol.* 37 (2003) 261.
33. S. Berto, F. Crea, P.G. Daniele, A. Gianguzza, A. Pettignano, S. Sammartano, *Coord. Chem. Rev.* 256 (2012) 63.
34. C. De Stefano, A. Gianguzza, T. Leggio, S. Sammartano, *J. Chem. Eng. Data* 47 (2002) 533.
35. C. De Stefano, A. Gianguzza, A. Pettignano, D. Piazzese, S. Sammartano, *J. Radioanal. Nucl. Chem.* 289 (2011) 689.
36. Y.S. Ho, G. McKay, D. a. J. Wase, C.F. Forster, *Adsorpt. Sci. Technol.* 18 (2000) 639.
37. Y.S. Ho, A.E. Ofomaja, *J. Hazard. Mater.* 129 (2006) 137.
38. Z. Xu, J.G. Cai, B.C. Pan, *J. Zhejiang Univ. Sci. A* 14 (2013) 155.
39. S. Cataldo, A. Gianguzza, M. Merli, N. Muratore, D. Piazzese, M.L. Turco Liveri, *J. Colloid Interface Sci.* 434 (2014) 77.
40. S.H. Ahmed, E.M. El Sheikh, A.M.A. Morsy, *J. Environ. Radioact.* 134 (2014) 120.
41. I. Twardowska, J. Kyziol, *Environ. Int.* 28 (2003) 783.
42. C. De Stefano, A. Gianguzza, D. Piazzese, S. Sammartano, *Anal. Bioanal. Chem.* 383 (2005) 587.

43. F. Crea, C. De Stefano, A. Gianguzza, A. Pettignano, D. Piazzese, S. Sammartano, *J. Chem. Eng. Data* 54 (2009) 589.
44. S. Sander, W. Wagner, G. Henze, *Anal. Chim. Acta* 305 (1995) 154.
45. T. Higuchi, *J. Pharm. Sci.* 52 (1963) 1145.
46. F. Langenbucher, *J. Pharm. Pharmacol.* 24 (1972) 979.
47. Y.S. Ho, J.F. Porter, G. McKay, *Water. Air. Soil Pollut.* 141 (2002) 1.
48. W.B. Xue, A.H. Yi, Z.Q. Zhang, C.L. Tang, X.C. Zhang, J.M. Gao, *Pedosphere* 19 (2009) 251.